GEOLOGICA CARPATHICA, APRIL 2023, 74, 2, 123–138 https://doi.org/10.31577/GeolCarp.2023.09

Assessment of the deformation in the subparallel shear zone set: A case study from the Veporic Unit, Western Carpathians

ROMAN FARKAŠOVSKÝ[1,✉], STANISLAV JACKO[1], ZDENKA BABICOVÁ[1] and ALEXANDER DEAN THIESSEN[1]

[1]Technical university in Košice, Faculty of Mining, Ecology, Process Control and Geotechnologies, Institute of Geosciences, Park Komenského 15, 042 00 Košice, Slovakia; ✉roman.farkasovsky@tuke.sk

(Manuscript received June 2, 2022; accepted in revised form March 29, 2023; Associate Editor: Rastislav Vojtko)

Abstract: During the Alpine convergence of the Central Western Carpathians, a set of subparallel NW–SE shear zones formed in the eastern part of the Veporic Unit, near the tectonic contact with the Gemeric Unit. Deformation in low-grade metamorphic conditions was typical of the Alpine movements in the shear zones. Mylonitic rocks of the crystalline complex and their cover formations were studied on a macro and micro scale to characterise the evolution of deformation structures in the shear zones. The differential stress of dynamically-recrystallized quartz, which aggregates in mylonitic rocks, was determined using quartz paleopiezometry. Several types of foliation structures, but mainly penetrative subhorizontal stretching lineation in all observed mylonites, provide evidence of stretching and oriented ductile flow in a NW–SE direction. Shear sense indicators show the subhorizontal movement of the shear zone hanging walls to the SE. Dynamically-recrystallized quartz aggregates in the mylonitic rocks show different values of grain sizes and differential stresses, depending on the structure in which they occur. The lowest differential stresses were found in the quartz aggregates parallel to the S planes of the mylonites. Higher values are related to the C shear bands. The character of the structural setting indicates the formation of the shear zones in the orogen-parallel extension conditions.

Keywords: shear zone, mylonite, microstructure, differential stress, quartz paleopiezometry, Western Carpathians

Introduction

Shear zones are tabular high-strain zones, which link tectonic contacts between two less strained or unstrained lithotectonic blocks (Ramsay & Graham 1970; Ramsay 1980; Lister & Snoke 1984; Passchier et al. 1990). They can be active during several stages of deformation (Bird et al. 2015; Phillips et al. 2016). Rocks in the shear zones can be deformed by brittle, brittle-plastic, or plastic deformation mechanisms. Brittle shear zones are dominated by grain fracturing, frictional sliding, and grain rotation deformation mechanisms. Dislocation creep, twinning, and diffusion are typical deformation mechanisms of plastic shear zones (Fusseis et al. 2006; Fossen & Cavalcante 2017). Crystal-plasticity during deformation depends on the mineral composition of deformed rocks, temperature, pressure, presence of fluids, strain rate, and grain size (Hirth & Tullis 1992; Paterson & Wong 2005; Fossen 2016; Papeschi et al. 2018). The temperature conditions needed for the transition from brittle to plastic deformation in quartz and feldspar rich rocks range from 300 to 450 °C (Scholz 1988; Stipp et al. 2002). The tectonites from this transition are typically composed of fractured feldspar porphyroclasts in a matrix of fine-grained recrystallized quartz (Viegas et al. 2016). Asymmetry of different types of porphyroclasts can be used for shear sense determination. At low-grade metamorphic conditions, quartz is deformed by dislocation and diffusion creep. Aggregates of dynamically-recrystallized grains develop and define typical foliation and stretching lineations in the mylonitic rocks. Dynamic recrystallization is related to changes in grain size, shape, and orientation of quartz grains. These quartz microstructures have so far proven to be useful records of deformation history (Stipp et al. 2004; Fitz Gerald et al. 2006). The above-mentioned structures and fabric elements were studied, and differential stresses were analysed using the quartz paleopiezometry method to characterize the deformation structure and development of the mylonitic rocks. Observations were made across the area of the subparallel set of shear zones near the contact of two Variscan basement units of the Central Western Carpathians. The deformation of shear zones varies with time as a result of gradual stress changes during their development. The system of shear zones formed during the northeast-vergent thrusting of the Gemeric Unit onto the Veporic Unit. Later, they were reactivated several times during their further tectonic development (Jacko et al. 2001; Jacko 2007). This deformation history had a significant impact on the present structure of the region.

Geological setting

The Central Western Carpathians consist of three major crustal units: from the south to the north, they are divided into

the Gemeric, Veporic, and Tatric units (Fig. 1). Each unit is composed of a Variscan basement with Upper Paleozoic to Mesozoic metasedimentary cover. On the eastern margin of the Central Western Carpathians, the Paleozoic complexes of the Gemeric Unit are separated from the Paleozoic complexes of the Veporic Unit by the Margecany shear zone. (Fig. 1b).

The eastern part of the Veporic Unit consists of a Variscan crystalline complex, Upper Paleozoic to Mesozoic cover formations, as well as isolated klippes of the Choč Nappe (Hronic Unit). The crystalline basement consists of three lithotectonic units (Fig. 2): the Lodina Complex, the Miklušovce Complex, and the Bujanová Complex, which are all separated by shear zones (Jacko et al. in Polák et al. 1997).

The Lodina Complex is formed mainly by gneisses, mica schists, and local lenses of amphibolites. T–P conditions of the Variscan metamorphosis did not exceed temperatures of 520–540 °C and a pressure of 300 MPa (Korikovskij et al. 1990). The Miklušovce Complex consists of migmatites, gneisses, and amphibolites, which are penetrated by younger bodies of aplite granites. The Variscan metamorphosis reached temperatures of 570–610 °C and pressures of 530–600 MPa (Korikovskij in Krist et al. 1992). The Bujanová Complex is mostly formed by granitoid rocks (Jacko in Polák et al. 1997; Bónová et al. 2010). The granitoid intrusions penetrate older fold structures of the complex. Metamorphic rocks, mainly gneisses, migmatites, and amphibolites participate in the Bujanová Complex's composition to a lesser extent. They are a product of the Variscan metamorphosis with temperatures between 620–625 °C and pressures between 400–450 MPa (Jacko et al. 1990). The cover formations of the Veporic Unit contain dynamically metamorphosed Carboniferous, Permian, and Early Triassic rocks, as well as unmetamorphosed Mesozoic rock sequences (Fig. 2). Detritic sediments are typical for the Late Carboniferous. Permian formations are composed of siliciclastic rocks and acidic volcanic rocks (Vozárová & Jacko in Polák et al. 1997).

The Mesozoic cover formations start with the transgressive Lower Triassic quartzitic psammites of the Lúžna Formation. Predominantly carbonate sedimentary rocks are typical of the Middle Triassic to the Late Jurassic period (Polák in Polák et al. 1997). Upper Paleozoic rocks of the Choč Nappe are tectonically reduced. They are formed by metasiliciclastic rocks, basaltic tuffs and diorite bodies (Vozárová & Vozár 1988; Vozárová in Polák et al. 1997). Lower Carboniferous rocks of the Gemeric Unit are present southwest of the Veporic Unit and the Margecany shear zone. They form a thick, volcano-sedimentary sequence represented by metasiliciclastic rocks and metabasites (Sasvári et al. in Polák et al. 1997).

The contact zone between the Gemeric and the Veporic units is formed by tectonic structures, which developed during several tectonometamorphic stages of the Variscan and Alpine orogenies (Jacko et al. 2001). The south-vergent nappe thrusting of the Miklušovce and the Bujanová complexes onto the Lodina Complex between 380–340 Ma had a significant impact on the Variscan structure. The syntectonic metamorphosis of this event reached P–T conditions of amphibolite facies. As a consequence of the Bujanová Complex emplacement, shear zones and foliation formed, dipping moderately

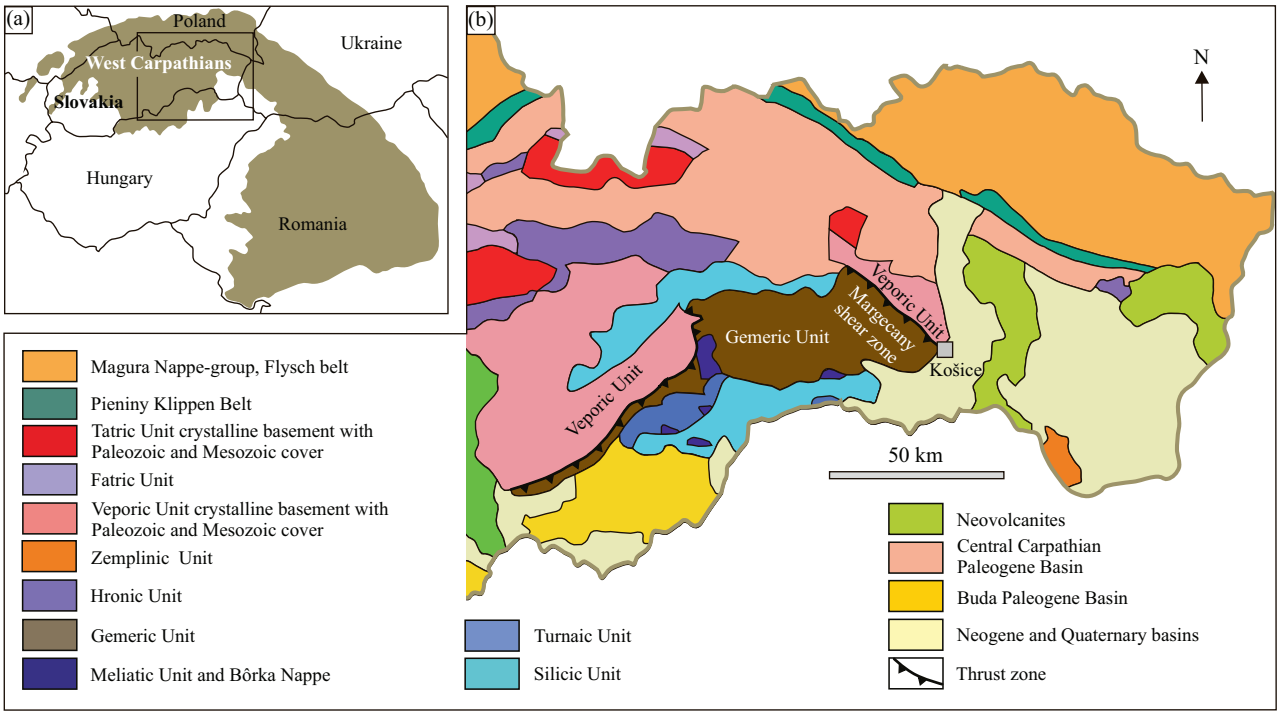

Fig. 1. a — Location of the Western Carpathians within the Carpathian arc. **b** — Tectonic map of the eastern part of the Western Carpathians with marked Margecany shear zone, which represents tectonic contact of the Gemeric Unit with the Veporic Unit (based on Biely et al. 1996).

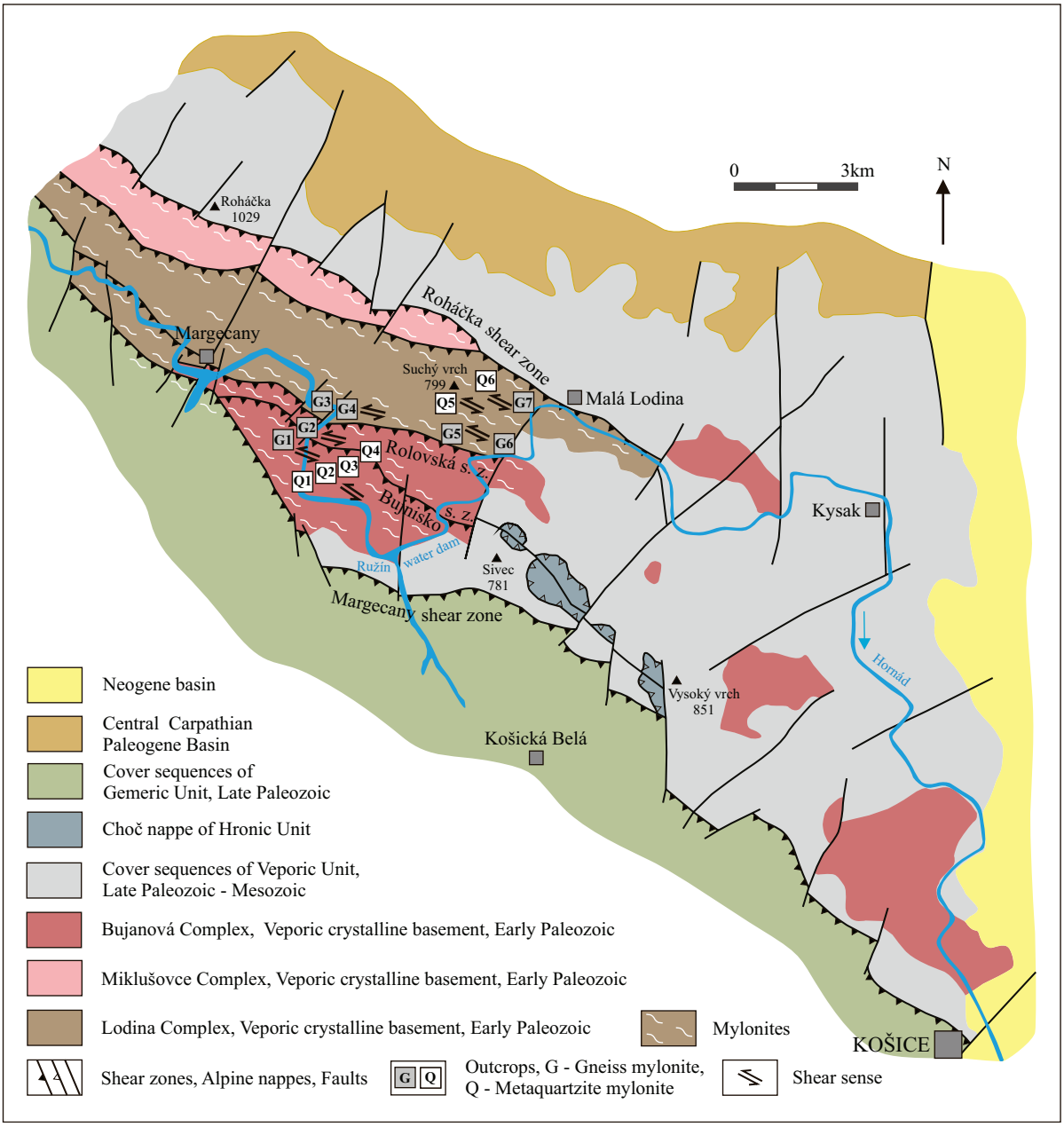

Fig. 2. Simplified tectonic map of the eastern part of the Veporic Unit between the towns of Košice and Margecany (modified after Polák et al. 1996). The subjects of the research were outcrops of mylonitic rocks, gneisses (G1–G7), and quartzites (Q1–Q6) in the system of the subparallel shear zones of the NW–SE direction.

to the SW. These shear zones later played a role during the development of the Alpine structures. Between 340–305 Ma granitoid bodies were intruded into the Miklušovce and Bujanová complexes (Jacko et al. 1996, 2001; Jacko 2007).

Alpine deformations in the contact area between the Gemeric and Veporic units had a multi-stage character and took place in low-grade metamorphic conditions (Korikovskij et al. 1989; Jacko 2007). NW–SE shear zones, which mostly dip to the SW, are characteristic features of the Alpine structure (e.g. Jacko et al. 1996; Farkašovský 2013; Farkašovský et al. 2016). In the region, the formation of the shear zones started with the progressive evolution of the orogenic front and the movements related to general north-south compression and northeast-vergent overthrusting of the Gemeric Unit onto the Veporic Unit.

In the western part of the Veporic Unit, overthrusting resulted in its burial between 108–95 Ma (Jeřábek et al. 2012; Bukovská et al. 2013). Cretaceous metamorphosis here reached maximum T–P conditions of 620 °C and 1.1 GPa (Janák et al. 2001). Folding of the deep Veporic crust, as well as the growth of the Veporic metamorphic core complex, was accompanied by upper crustal detachment faulting and eastward unroofing

of the Veporic Unit in its western part during the late Cretaceous (Plašienka et al. 2007; Jeřábek et al. 2012; Vojtko et al. 2016).

Final movements of a subhorizontal strike-slip character in the brittle-ductile regime were described in the shear zones in the eastern part of the Veporic Unit (Jacko et al. 2001; Jacko 2007). The system of shear zones in the Veporic Unit, which is subparallel with the Margecany shear zone (Fig. 2), separates the crystalline complexes and the cover formations of the Veporic Unit from each other. Slices of the Lower Triassic quartzites of the Lúžna Formation and rauwacks of the Middle to Upper Triassic dolomites are rooted in them. At the surface, they form mylonite zones 10 to 100 m thick (Fig. 2), which are markedly segmented by the transverse faults.

Methods

The mylonite outcrops in the shear zones (G1–G7 and Q1–Q6; Fig. 2) were first studied macroscopically. That study aimed to identify the structure of the mylonitized rocks. The geometrical parameters (dip direction and dip angle) of the foliation and stretching lineation were measured. Structural data were displayed and evaluated in TectonicsFP 1.7.8 software using lower hemisphere projection. Afterwards, oriented samples were collected from selected points. For the microscopic study, oriented thin sections were prepared in the planes parallel to the stretching lineation and normal to the mylonitic foliation. Microscopic observations were made using a petrographic polarising microscope, Olympus BX53 with a Promicam 3-3CP camera.

The mylonites were assessed according to their original lithotype (gneiss mylonite G1–G7, quartzite mylonite Q1–Q6). The mylonites were further classified according to their porphyroclasts/matrix ratio (Sibson 1977). The microfabric (cleavage, microfolds, porphyroclasts, fragmented grains) and shear sense of the mylonites were assessed (Passchier & Trouw 2005).

The method of quartz paleopiezometry was applied for the determination of differential stresses ($\sigma_D=\sigma_1-\sigma_3$; MPa). The size of dynamically-recrystallized grains in deformed rock relates to differential stress, which has previously been proven by several authors (e.g. Mercier et al. 1977; Twiss 1977; Christie et al. 1980; Schmid et al. 1980; Etheridge & Wilkie 1981; Michibayashi 1993; Post & Tullis 1999; Passchier & Trouw 2005). This method is most applicable for rocks and mineral aggregates, which are composed predominantly of quartz with pervasive ductile deformation. The numeric determination of differential stresses in MPa takes into account the size of the dynamically-recrystallized grains. The primary data were obtained from oriented thin sections. To guarantee the most representative data, the thin sections were analysed by systematically measuring grain sizes in quartz aggregates. The longer diameters of individual quartz grains were measured in photomicrographs and recorded in the tables using QuickPHOTO Camera 3.2 software for digital photomicrography, image editing, and measurements. To determine differential stress values, the software program GrainSizeTool (an open-source, cross-platform script written in Python) (Lopez-Sanchez 2018) was used. Grain size populations were visualized. Differential stresses were estimated via a quartz paleopiezometer (Twiss 1977; Stipp & Tullis 2003; Lopez-Sanchez & Llana-Fúnez 2015).

Results

Macroscopic structure of the mylonites

Macroscopically, the studied rock samples within the shear zones can be divided into two groups. The first group is represented by gneiss mylonites of the Veporic crystalline complex, which are mainly composed of quartz, feldspars, and mica. S–C fabric is a typical structure of these rocks (Fig. 3a, b) and is mainly visible at a microscopic scale. Macroscopically, only one system of foliation planes is dominant in most cases – the system of S-planes (Fig. 3d). Both foliation planes predominantly dip to the S-SW and they are subhorizontal only in certain places (Fig. 4a).

The second group of rocks are the quartzite mylonites from the cover formations of the Veporic Unit. These mylonites are predominantly composed of quartz agregates. They are represented by one dominant system of foliation planes which have a variable dip. Deformation of metaquartzite by folding is scarce. They have a slight to medium dip southwestwards, and they are occasionally subhorizontal (Fig. 4c).

All of the foliation planes of the gneiss mylonites contain visible subhorizontal stretching lineations, which are oriented in a NW–SE direction (Figs. 3c, 4a, b). Most lineations dip slightly towards the southeast (Figs. 3c, 4b). In the case of quartzite mylonites, the lineations can be slightly inclined on both sides (Fig. 4c, d). Stretching lineations are a characteristic structural element of all the mylonites in the area. They restrict the movement of the shear zones in the area towards a NW–SE direction during the final stages of ductile deformation.

Determining the sense of shear in the macroscale is only possible in cases where geometrical relationships of the S and C planes in gneiss mylonites are identifiable (Figs. 3a, 4a). The effect of shear can also be determined from asymmetrically deformed objects, such as quartz lenses (Fig. 3b). Based on these indicators, as well as asymmetric indicators on a microscale, the overlying blocks of the shear zones moved from the top towards the southeast (Fig. 4a, c).

Microfabric of the gneiss mylonites

Gneiss mylonites developed by multiple deformations (outcrops G1–G7). The Variscan crystalline rocks with an oriented metamorphic structure were involved in the deformation process. In terms of microfabric, there is a characteristic bimodal grain size distribution in the gneiss mylonite. The matrix is distributed among larger grains of quartz, feldspar, and mica

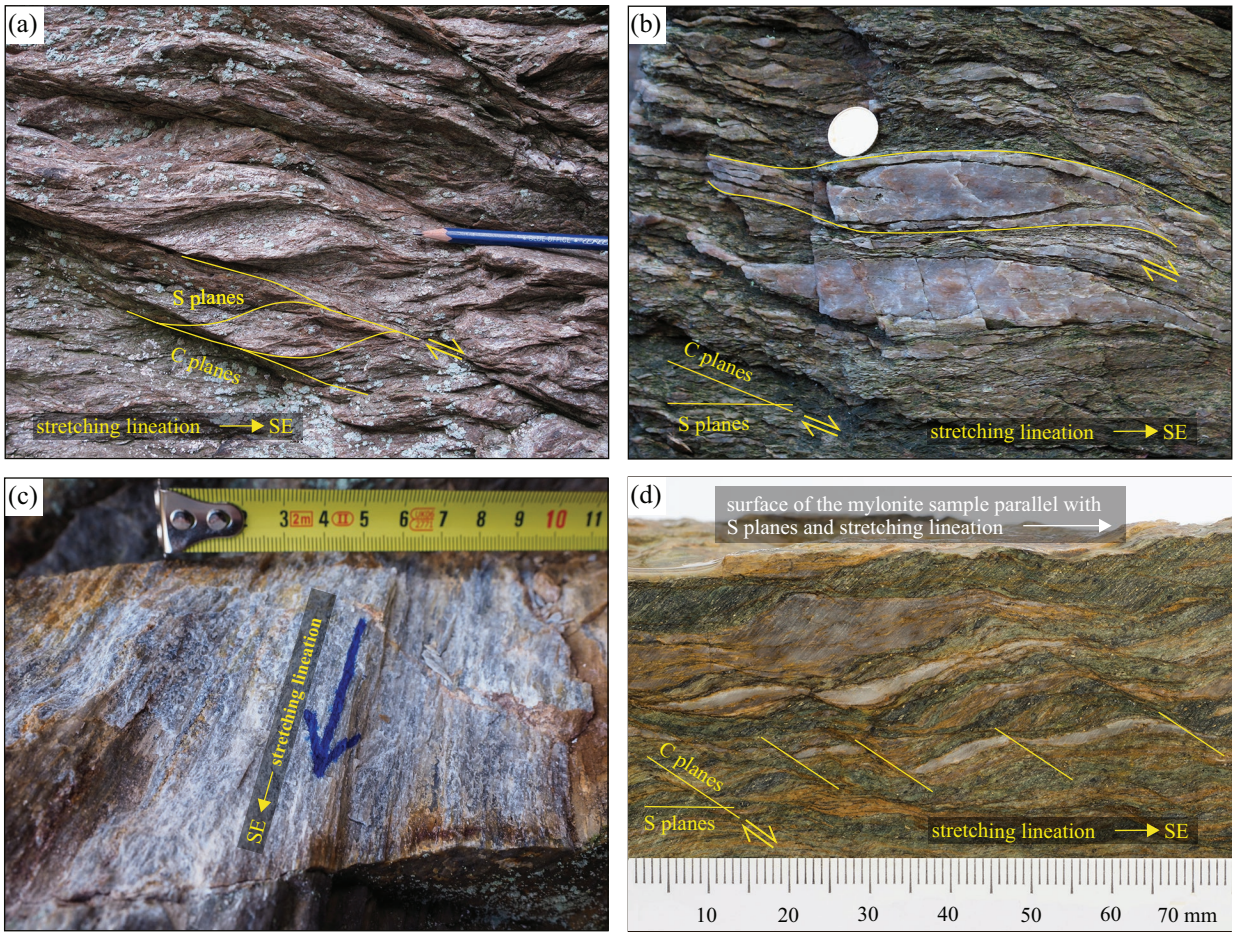

Fig. 3. Field photographs: **a** — mylonite of the gneissic rock with macroscopic shear band cleavage and asymmetric bending of the foliation among the shear bands, asymmetry of the shear sense markers indicate top to the SE movement (outcrop G4); **b** — deformed asymmetric lenses of the quartz in gneiss mylonite, asymmetry of the shear sense markers shows top to the SE movement (outcrop G5); **c** — trace of the stretching lineation in the gneiss mylonite (outcrop G3); **d** — cross-section of the oriented mylonite sample (outcrop G2) parallel with stretching lineation and perpendicular to S planes (mylonite foliation).

porphyroclasts. It is formed by aggregates of small grains of approximately uniform size, which are oriented parallel to the S planes (Fig. 5). The mylonites of the gneissic rocks fall under the category of mesomylonites (65–85 % of the matrix).

Foliation is a characteristic feature of the mylonites on a micro scale. In many cases, two sets of foliation planes developed: planes of shear bands (C planes) and older, pervasive foliation (S planes), which are deformed by the shear bands. Both planar systems form shear band cleavage (Gapais & White 1982) or a so-called C/S fabric (Berthé et al. 1979; Lister & Snoke 1984). S planes are generally formed by elongated-oriented aggregates of mica, as well as by aggregates of dynamically-recrystallized quartz that define the stretching lineation. Syntectonic fine-grained sericite aggregates of the S-planes are deflected near the porphyroclasts and bent near the shear bands (Fig. 5). The quartz creates aggregates of dynamically-recrystallized, small, elongated grains. Original quartz porphyroclasts with strong undulose extinction form subgrains at the edges. The subgrains have a similar size and orientation like newly-formed grains, which are a part of aggregates of dynamically-recrystallized quartz. Shear bands (C planes) that form shear band foliation are a characteristic fabric element of the mylonites. In terms of shear band orientation, the shear bands parallel and oblique (Berthé et al. 1979) to the shear zone boundary are present. They are short, tight, and penetrative and they are formed by the fine-grained aggregates of quartz and chlorite. S planes in the microlithons are curved near the shear bands (Fig. 5a–d). The asymmetry of the shear band's foliation indicates the movement top-to-the-SE along with the shear bands (Fig. 5a–d). Shear band foliation can be partially overprinted by younger sets of shear bands with an identical effect of shear and noticeably thicker domains. The younger sets of shear bands make a smaller angle with the S foliation than the older ones. Younger shear bands change their thickness laterally and are spaced relatively further apart from each other.

S foliation planes are deformed by isoclinal or tight microfolds (Fig. 5c, d). Their profile planes are perpendicular to foliation planes and parallel to NW–SE stretching lineation. Axial planes of the microfolds are generally oriented

subparallel to S foliation. In most cases, only the relics of microfold hinges and adjacent limbs were preserved. The microfolding in the gneisses was rather local. Microfolds, which developed during extensional shear deformations, have been described previously by several authors (Berthé et al. 1979; Platt & Vissers 1980; Passchier & Trouw 2005). The folded planes are mainly formed by oriented aggregates of sericite, chlorite, or dynamically-recrystallized quartz. Microfolds are transected by the younger shear band structures (C planes).

Porphyroclasts are represented by minerals that are more resistant to deformation or dynamic recrystallization than the mineral grains in the matrix. The grains of the porphyroclasts are considerably bigger than the grains forming the matrix. The porhyroclasts in the mylonites belong to pretectonic crystals, which had formed in the rocks before the deformation started. Most often, porhyroclasts are formed by feldspars and quartz (Fig. 5b, c, e, f). Pre-tectonic crystals are usually deformed. Undulose extinction and deformation lamellae, which are evidence of crystal lattice distortion, are

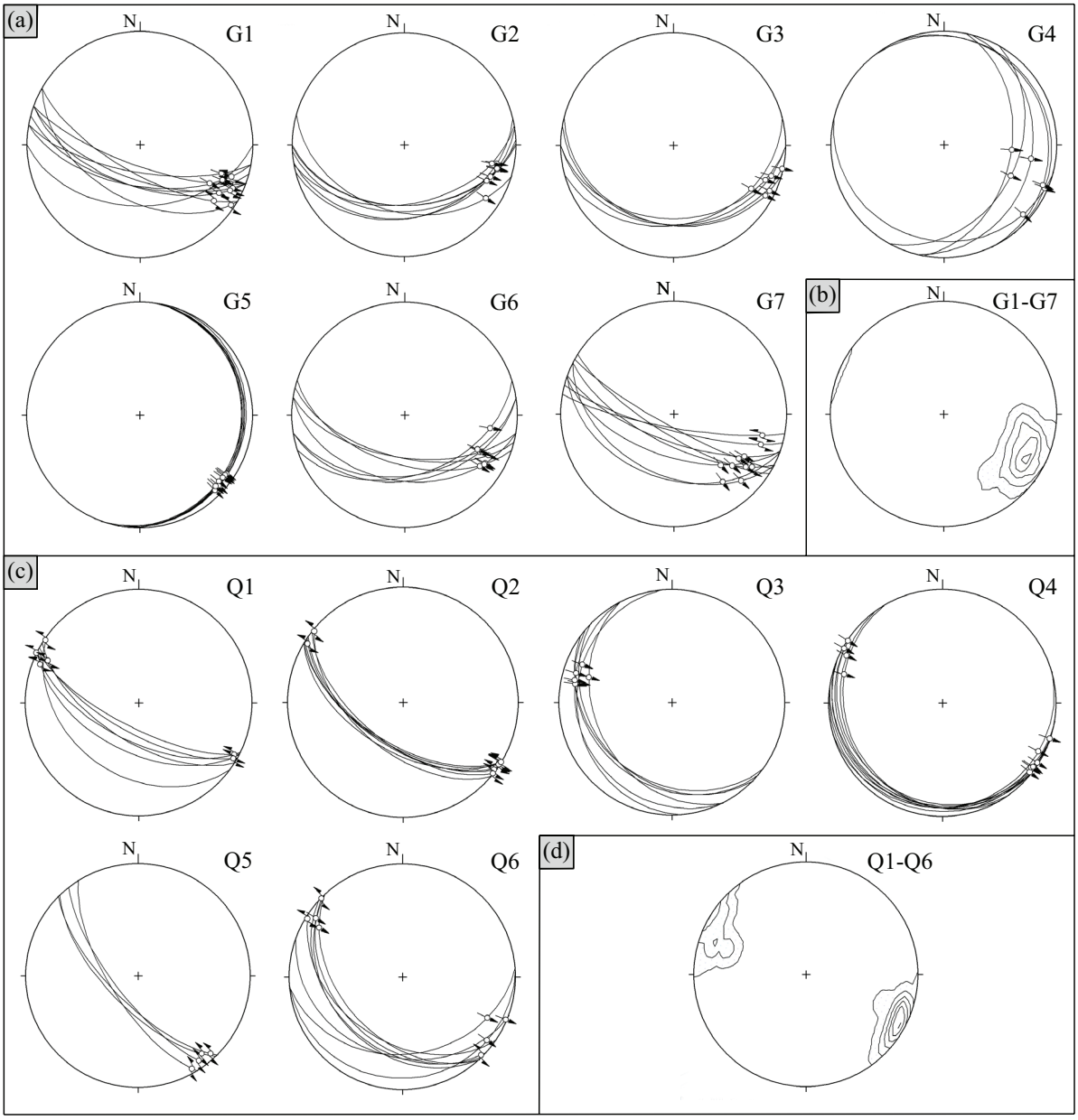

Fig. 4. Foliation and lineation of main structures documented in the field (Lambert projection, lower hemisphere): **a** — tectonograms of the foliation S planes and the stretching lineations in the gneiss mylonites; **b** — contour diagram of the stretching lineations slightly dipping to the SE in the gneiss mylonites; **c** — tectonograms of the foliation planes and the stretching lineations in the metaquartzite mylonites; **d** — contour diagram of the NW–SE subhorizontal stretching lineations in the metaquartzite mylonites; top to the SE sense of shear on the planes was determined by macroscopic, as well as microscopic observations.

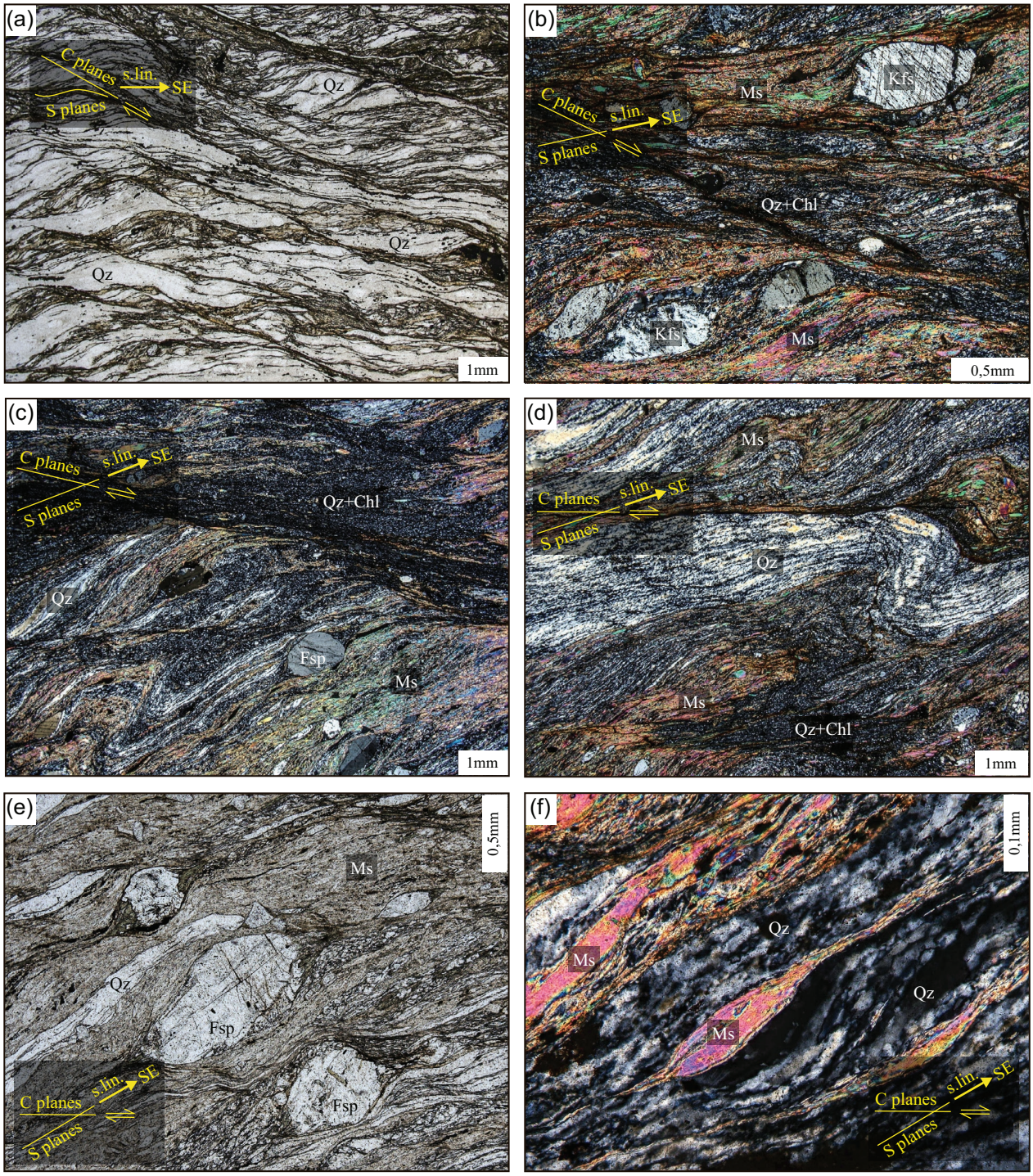

Fig. 5. Microstructures in the crystalline gneiss mylonites, top to the SE effect of the shear: **a** — relationship of the C and S planes in the C/S fabric, S planes, which are formed mainly by dynamically-recrystallized quartz ribbons, are asymmetrically-curved near the C planes (outcrop G5, PPL); **b** — C planes transecting older S foliation, asymmetric feldspar porhyroclasts are present parallel to S foliation (outcrop G2, CPL), **c** — typical microfabric of the mylonites with σ-type feldspar porphyroclasts and relics of tight to isoclinal microfolds parallel to S foliation (outcrop G3, CPL); **d** — microfold formed by dynamically recrystallized quartz ribbon with limbs parallel to S foliation transected by the C plane (outcrop G7, CPL); **e** — asymmetric sigma porphyroclasts with feldspar core and the tails formed by quartz and chlorite aggregates (outcrop G1, PPL); **f** — muscovite mica fish in the aggregates of dynamically-recrystallized quartz (outcrop G6, CPL). Note: PPL – plane-polarized light, CPL – crossed polarized light, s.lin – stretching lineation.

typical of quartz. Porphyroclast grains can be fragmented or boudinaged. Deformation, bending, or deflection of the foliation planes is common near them. In the mylonites of gneisses, white mica fish are typical. Most often, they can be classified as group 1 (ten Grotenhuis et al. 2003). Asymmetry of the mica fish microstructures indicates the movement of the shear zone hanging walls from the top to the SE (Fig. 5f). Core and mantle microstructures are often formed around the K-feldspar porphyroclasts and less so around plagioclase and quartz porphyroclasts. Asymmetric mantles were formed near the periphery of the porphyroclast during ductile deformation. Asymmetric core and mantle structures (mantled porphyroclasts) almost exclusively belong to σ-type objects (Fig. 5b, c, e) based on the classifications of Passchier & Simpson (1986); Passchier & Trouw (2005). For the tail parts, a soluble mineral association of quartz and chlorite is typical. The Asymmetry of the core and mantle microstructures indicates the movement of the shear zone hanging walls from the top to the SE.

Fragmented mineral grains and microfaults in the mylonites of the gneissic rocks are less common. Microfault forming is most often joined with rheologically-rigid feldspar grains. However, the presence of microfaults are less common in micas, where the formation of microstructures is related to sliding on (001) crystallographic planes. In most cases, development of the microfractures in the feldspar porphyroclasts is connected with shear zone exhumation when deformed rocks reach higher crustal levels (Pryer 1993; Guermani & Pennacchioni 1998).

Microfabric of the mylonitized Lower Triassic metaquartzites

Metaquartzites and quartzose metasandstones overlie the areas of Pre-Mesozoic units. At present, contact with underlying rocks is usually tectonic. Undeformed metaquartzites and quartzose metasandstones are pale-grey to pink layered rocks. The clastic material is formed mainly by angular to subangular quartz grains (85–89 %) and less so by feldspar and muscovite (Polák et al. 1997). While the mylonitized metaquartzites are mainly composed of quartz, their microfabric is quite monotonous. They were substantially dynamically recrystallized. In terms of microfabric, bimodal grain size distribution is characteristic, with large grains of quartz surrounded by aggregates of small quartz grains, which are oriented parallel to foliation and stretching lineation (Fig. 6b, c, d). The original quartz grains have undulose extinction in their central parts and form subgrains at the edges (Fig. 6b, c). The dynamic recrystallization leads to an approximately uniform size, as well as a uniform orientation of the newly-formed quartz grains in the matrix aggregates. This was caused by deformation and recrystallization at specific differential stress (Fig. 6a). The size of the recrystallized grains and subgrains is proportional to the value of differential stress (Chester 1989). Sometimes, shear band structures are present in the mylonitized metaquartzites. Shear bands are non-penetrative and are usually short and tight. Relics of microfold hinges and the adjacent limbs are only occasionally preserved (Fig. 6d). Microfolding has only a local character. The asymmetry of the microstructures indicates the movement of the shear zone hanging walls from the top to the SE (Fig. 6b, c).

Paleopiezometry of the mylonitized rocks

One of the defining characteristics of the Veporic shear zone's mylonites is aggregates of dynamically-recrystallized quartz grains with a preferred orientation. Changes in grain size, shape, and orientation are typical of dynamic recrystallization. The formation of new grains reduces the internal strain energy associated with increased dislocation density (Stünitz 1998). In experiments with quartz deformation, three dislocation creep regimes are present (Hirth & Tullis 1992). At high-stress levels, new grains form by the bulging of grain boundaries (regime 1). At moderate stress, new grains are formed mainly by subgrain rotation recrystallization (regime 2). At low stress (regime 3), recrystallized grains form by both grain-boundary migration recrystallization and subgrain rotation recrystallization (Stipp & Kunze 2008). Subgrain rotation recrystallization shows the gradual lateral transition of subgrains into aggregates of newly formed grains, which have approximately the same size. This is typical of these studied gneiss and metaquartzite mylonites. Bulging of the grain boundaries was observed only to a lesser extent. For this reason, Twiss's (1977) and Stipp & Tullis's (2003) methods (both are suitable for regimes 2 and 3) were used for the calculation of differential stresses (Lopez-Sanchez 2018). The use of two methods enables comparison and control of the obtained results simultaneously.

Dynamic recrystallization behaves differently in the mylonitic gneisses of the basement crystalline units in comparison with the metaquartzite mylonites of the cover formations. The average size of the quartz grains in the undeformed gneisses was from 0.5 to 1.5 mm. Mylonites of the gneisses (outcrops G1–G7; Fig. 2) are less homogeneous when it comes to mineral composition and microfabric. The various dynamically-recrystallized aggregates are parallel to the mylonite's different planar and linear elements. Coarse-grained aggregates, with an average quartz grain size of 37.31–42.09 μm (Figs. 7, 8; Table 1), are oriented parallel to the S foliation planes. These represent original quartz ribbons that have been dynamically recrystallized. Here, differential stresses reach minimum values of 35.63–38.68 MPa (Twiss 1977) or 33.57–37.12 MPa (Stipp & Tullis 2003). In wider, unequally distributed dynamically-recrystallized zones near the shear bands, quartz grains reach sizes of 20.46–22.46 μm (Figs. 7c, 8; Table 1). These have differential stresses of 55.00–58.19 MPa (Twiss 1977) or 54.30–59.76 MPa (Stipp & Tullis 2003). The smallest dynamically-recrystallized quartz grains in aggregates were observed in areas of the sharply-bounded, wide shear bands. Quartz grains here reach sizes of 14.89–16.89 μm (Figs. 7, 8; Table 1). These also have the highest recorded differential stresses of 66.01–72.23 Mpa (Twiss 1977) and 69.01–76.25 MPa (Stipp & Tullis 2003). Since the S foliation

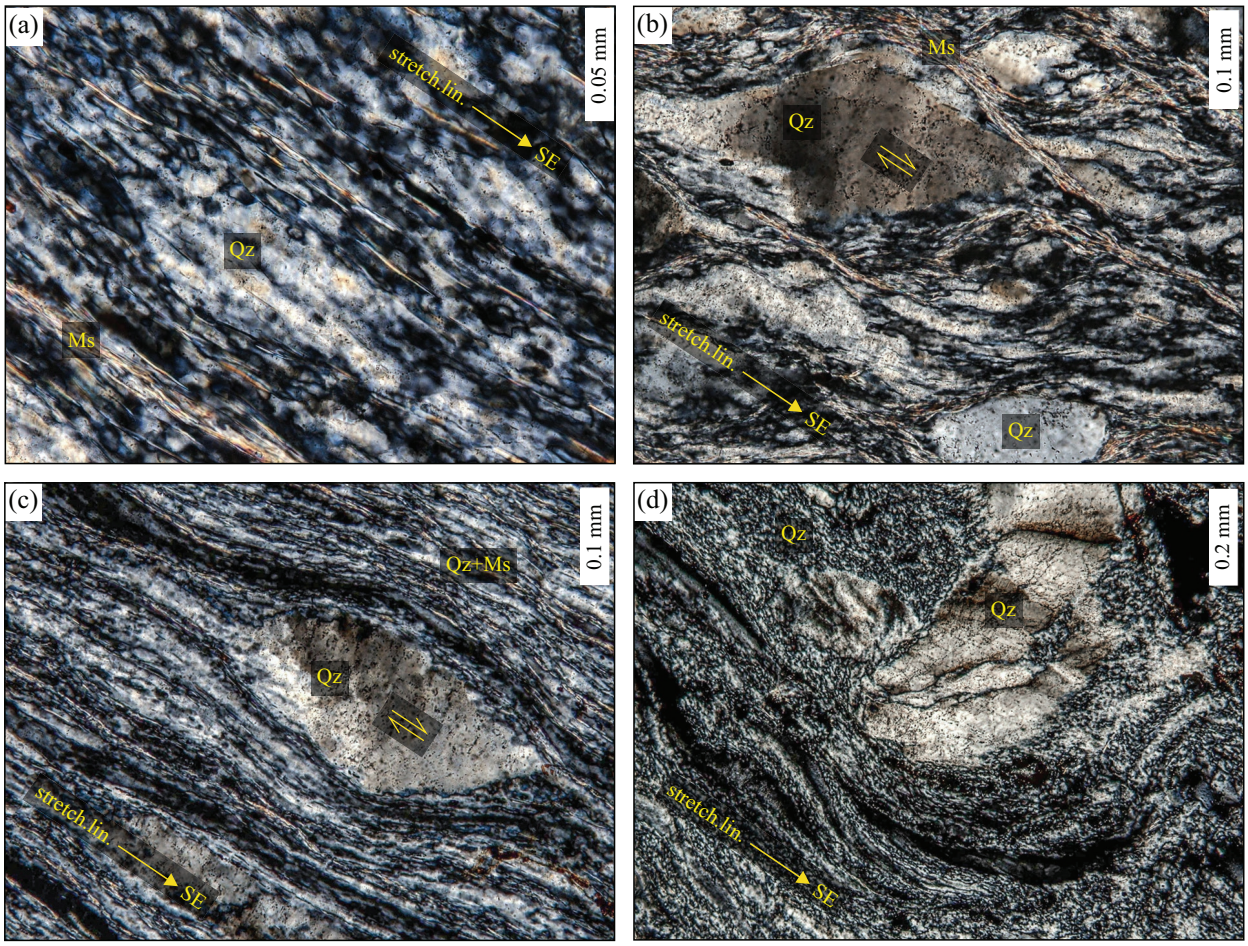

Fig. 6. Microphotographs of the quartzite mylonites of the Veporic Unit cover formations (Early Triassic), top-to-the-SE effect of the shear: **a** — aggregates of dynamically-recrystallized quartz and small mica grains oriented parallel to foliation and stretching lineation (outcrop Q4, CPL); **b** — asymmetric porphyroclast of quartz with undulose extinction bounded by short anastomosing shear bands, oriented mineral aggregates in the microlihton are bent near the shear band, (outcrop Q6, CPL); **c** — bimodal grain size structure, with large undulose quartz grain (porphyroclast) surrounded by oriented aggregates of small quartz grains (outcrop Q3, CPL); **d** — relics of microfolds formed by oriented aggregates of dynamically-recrystallized quartz (outcrops Q5, CPL). Note: CPL – crossed polarized light.

planes represent older structural elements than C shear bands, it is possible to conclude that the amount of differential stress in gneiss mylonites progressively rose as deformation progressed, and movements concentrated in the shear band domains.

From a structural standpoint, metaquartzite mylonites (outcrops Q1–Q6; Fig. 2) are more homogeneous when compared to gneiss mylonites. Their microstructure is simpler, since in most cases, they contain only one system of foliation planes (Fig. 6). They typically contain asymmetric, slightly-flattened quartz porphyroclasts with undulose extinction and sutured grain boundaries in a foliated fine-grained matrix (Fig. 6b, c). The average size of the quartz porhyroclasts is from 0.1 to 1.2 mm. The size of the quartz grains in the undeformed quartzite was up to 2.0 mm. Based on microfabric features, deformation in low-temperature conditions can be assumed. The rocks are formed mainly by quartz and, to a small extent, white mica. The average sizes of quartz grains in dynamically-recrystallized aggregates are 14.86–16.58 μm (Fig. 9; Table 1). The differential stress values of 67.14–72.33 MPa (Twiss 1977) and 70.38–76.36 MPa (Stipp & Tullis 2003) were calculated. The size of the quartz grains and the differential stress values in the aggregates of the dynamically-recrystallized quartzite mylonite are equivalent to the values which were recorded in wide shear bands of the mylonitic gneisses (Table 1).

Discussion

The tectonic zone, which separates the Variscan Gemeric and Veporic units in the eastern part of the Central Western Carpathians (Figs. 1, 2) represents a suitable example of multistage evolution documented by a variety of deformation processes and structures. One major structure, the Lubeník–Margecany shear zone, was formed during the Alpine

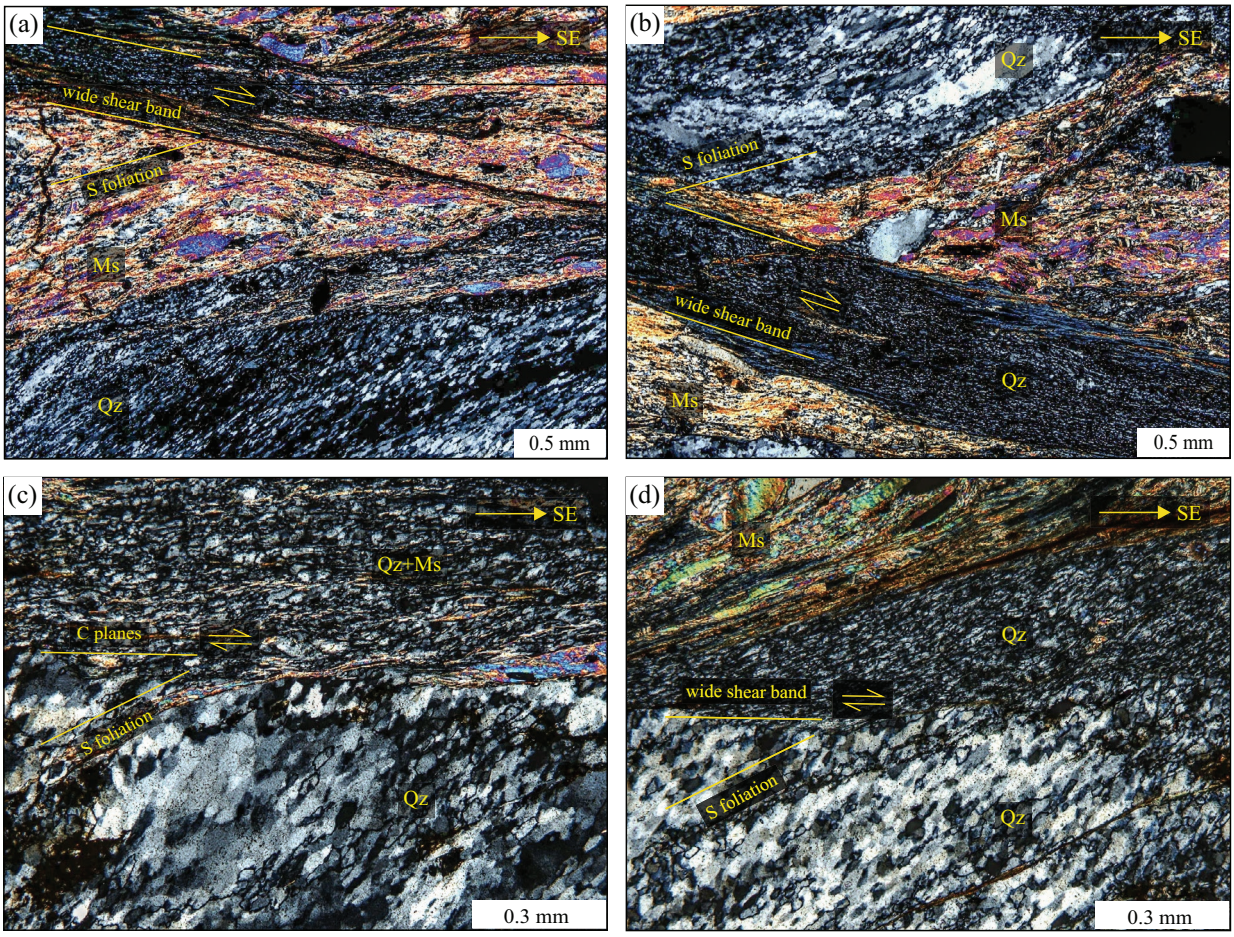

Fig. 7. Examples of the dynamically recrystallized aggregates with the different average sizes of quartz grains in the mylonites of the gneisses, top to the SE effect of shear: **a** — coarser-grained quartz aggregates (approx. 40 μm) parallel to S foliation and finer-grained aggregates (approx. 15 μm) in the wide shear band (outcrop G1, CPL); **b** — the wide shear band with sharp boundaries filled with fine-grained quartz aggregates (approx. 16 μm), coarser-grained aggregates of quartz (approx. 41 μm) and white mica forming S planes are bent near the shear band (outcrop G4, CPL); **c** — detailed view of the contact of the S foliation with coarser-grained quartz aggregates (approx. 41 μm) with the finer-grained quartz aggregates (approx. 22 μm) (outcrop G7, CPL); **d** — detailed view of the contact of the coarser-grained quartz aggregates (approx. 37 μm) of the S foliation with the finer-grained quartz aggregates (approx. 15 μm) in the wide shear band (outcrop G6, CPL). Note: CPL – crossed polarized light.

Cretaceous north-south shortening of the Central Western Carpathians (Plašienka 1995, 2003; Lexa et al. 2003; Jeřábek et al. 2012) and is represented in the east by the northeast-vergent thrusting of the Gemeric Unit onto the Veporic Unit (Jacko 2007). Due to the shortening, both superficial and basement nappes were formed. Superficial nappes were thrust a greater distance. Displacement in the basement was accompanied by shear zone formation. After northeast-vergent thrusting, uplift of the Veporic crystalline complex began with subsequent extensive unroofing of the Veporic Unit during the Late Cretaceous (Plašienka et al. 2007; Vojtko et al. 2016). Unroofing with hanging walls sliding back to the southwest was described in the eastern part of the contact zone between the Gemeric and Veporic units (Németh et al. 2000). The next stage of deformation caused brittle-ductille reactivation of the shear zones with subhorizontal strike-slip kinematics (Jacko et al. 1996, 2001; Jacko 2007).

The structural result is a set of parallel shear zones formed northeast of the Margecany shear zone in the Veporic Unit. Similar mylonite zones located close to each other at a distance less than 10 km from the Margecany shear zone are not present in the adjacent part of the Gemeric Unit in the southwest (Fig. 2). NW–SE shear zones are perpendicular to the direction of Alpine thrusting (e.g., Lexa et al. 2003). Mylonites in the shear zones of the Veporic crystalline complex have penetrative subhorizontal stretching lineation of a NW–SE direction (Figs. 3c, 4). The orientation of the lineation, defined mainly by the oriented quartz and mica aggregates, indicates that mylonites of the crystalline rocks, as well as metaquartzites underwent stretching and oriented ductile flow in a NW–SE direction parallel to the Alpine lithotectonic units and shear zones of the region. Microscopic, as well as macroscopic shear sense indicators show consistent top-to-the-SE subhorizontal movement of the shear zone hanging walls

sample	Sizes of quartz grains parallel to S foliation 37.31 - 42.09 μm	 parallel to C planes 20.46 - 22.46 μm	 inside the wide shear bands 14.89 - 16.89 μm
G1	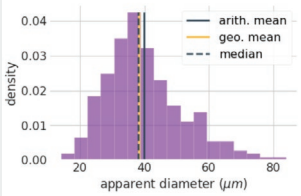	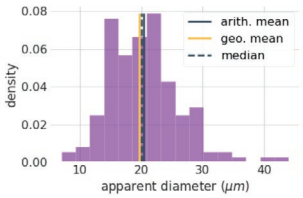	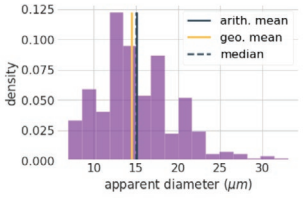
G2	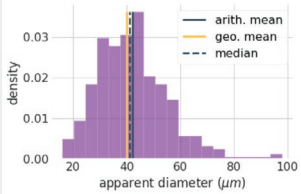	no measurements	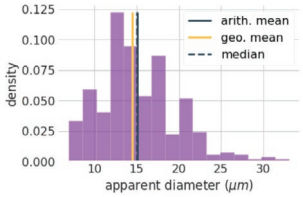
G3	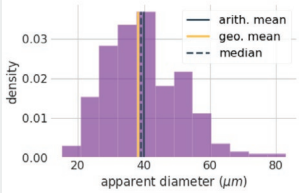	no measurements	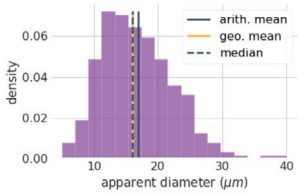
G4	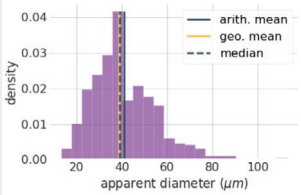	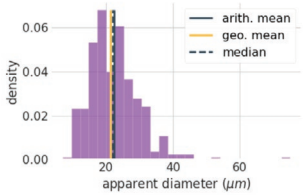	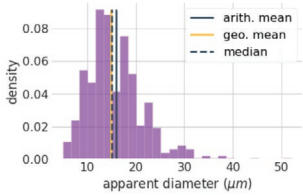
G5	no measurements	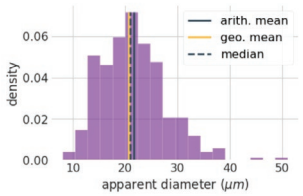	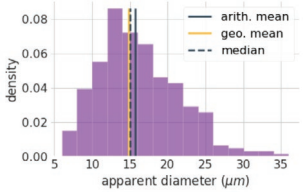
G6	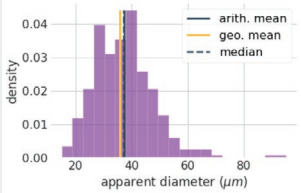	no measurements	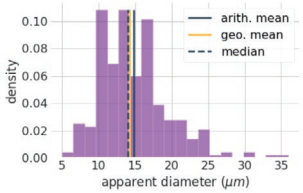
G7	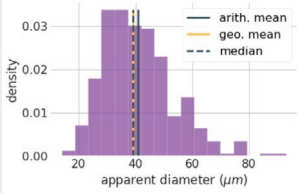	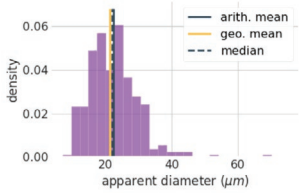	no measurements

Fig. 8. Distribution of the quartz grain sizes in the dynamically-recrystallized aggregates of the gneiss mylonites.

Table 1: Average sizes of quartz grains and corresponding differential stress in the samples of gneiss mylonites (G1–G7) and quartzite mylonites (Q1–Q6) due to the structural position.

Gneiss mylonites									
Outcrop sample	Dynamically recrystallized quartz aggregates in S planes			Dynamically recrystallized quartz aggregates near C shear bands			Dynamically recrystallized quartz aggregates in wide C shear bands		
	Average size of quartz grains (μm)	Differential stress (Mpa) (Twiss 1977)	Differential stress (Mpa) (Stipp & Tullis 2003)	Average size of quartz grains (μm)	Differential stress (Mpa) (Twiss 1977)	Differential stress (Mpa) (Stipp & Tullis 2003)	Average size of quartz grains (μm)	Differential stress (Mpa) (Twiss 1977)	Differential stress (Mpa) (Stipp & Tullis 2003)
G1	39.85	36.98	35.18	20.46	58.19	59.76	–	–	–
G2	42.09	35.63	33.57	–	–	–	15-Nov	71.51	75.67
G3	39.79	36.89	35.28	–	–	–	16.89	66.01	69.01
G4	40.74	36.27	34.20	22.46	55.39	54.84	15.97	68.78	71.13
G5	–	–	–	21.58	56.12	57.19	15.72	69.61	72.57
G6	37.31	38.68	37.12	–	–	–	14.89	72.23	76.25
G7	40.89	36.34	34.39	22.23	55.00	54.30	–	–	–
Quartzite mylonite									
Outcrop sample							Dynamically recrystallized quartz aggregates		
	Average size of quartz grains (μm)	Differential stress (Mpa) (Twiss 1977)	Differential stress (Mpa) (Stipp & Tullis 2003)	Average size of quartz grains (μm)	Differential stress (Mpa) (Twiss 1977)	Differential stress (Mpa) (Stipp & Tullis 2003)	Average size of quartz grains (μm)	Differential stress (Mpa) (Twiss 1977)	Differential stress (Mpa) (Stipp & Tullis 2003)
Q1	–	–	–	–	–	–	16.55	67.22	70.03
Q2	–	–	–	–	–	–	16.58	67.14	70.38
Q3	–	–	–	–	–	–	15.74	69.55	73.84
Q4	–	–	–	–	–	–	16.55	67.22	69.40
Q5	–	–	–	–	–	–	14.86	72.33	76.36
Q6	–	–	–	–	–	–	15.31	70.88	75.48

(Figs. 3a, b, 4a, c, 5, 6b, c), while some authors described opposing movements (Gazdačko 1994).

Another approach to the development of the above-mentioned structures provides a concept of orogen-parallel extension that was described in several continental collisional orogens (Ellis & Watkinson 1987; Dewey et al. 1988; Burg et al. 1994). The orogen-parallel extension, which was accompanied by horizontal ductile flow and stretched in an east–west direction parallel to the strike of the Cretaceous Western Carpathian orogen, were documented in the western part of the Veporic Unit (Jeřábek et al. 2007). The process can also be associated with the lateral escape connected to the thrusting of rheologically-weaker blocks between strong thrust sheets (Indares et al. 2000) and syn-convergent exhumation of buried crustal rocks (Ratschbacher et al. 1991; Mancktelow & Pavlis 1994; Janák et al. 2001). The Veporic Unit is considered to be the low-viscosity weak part between the southern Gemeric and northern Tatric units (Plašienka 2003). Progressive burial of the Veporic crust, simultaneously with the orogen-parallel ductile spreading, occurred during the overthrusting of the Gemeric Unit from the south, with underthrusting of the Tatro–Fatric basement from the north (Jeřábek et al. 2007). Orogen-parallel flow in this area occurred with an increase in pressure and temperature, contemporaneously with burial (Jeřábek et al. 2008).

Alpine mylonitization in the eastern part of the Veporic Unit (Korikovskij et al. 1989), as well as in the western part of the Veporic Unit (Putiš et al. 1997), occurred in the low-grade metamorphic conditions. In the Lodina Complex, which is the Variscan tectonic footwall of the overlying Bujanová Complex, mylonites with a higher matrix content are present. Mylonites with a lower matrix content are typical of the Bujanová Complex. Microstructures indicate a slight increase in mylonitization towards the structural footwall, which coincides with observations in the western part of the Veporic Unit (Jeřábek et al. 2007).

At low grade metamorphic conditions, feldspar deformation is still brittle, whereas quartz is deformed ductilely (Simpson 1985). Quartzo-feldspathic mylonites of the eastern part of the Veporic Unit contain angular porphyroclasts of the feldspars deformed by brittle fracturing. Undulose extinction and deformation lamellae are typical of the quartz porphyroclasts (Fig. 6b, c, d). These microstructures are characteristic at temperatures of 300–400 °C (Pryer 1993). Core-and-mantle structures (Fig. 5b, c, e), with a feldspar core and a sharp boundary with a mantle of fine-grained mineral aggregates, are also present at temperatures of 400–500 °C (Pryer 1993; Passchier & Trouw 2005). Subgrains form in the original quartz grains, which pass laterally to aggregates of newly-formed, dynamically-recrystallized quartz. Deformation microstructures of

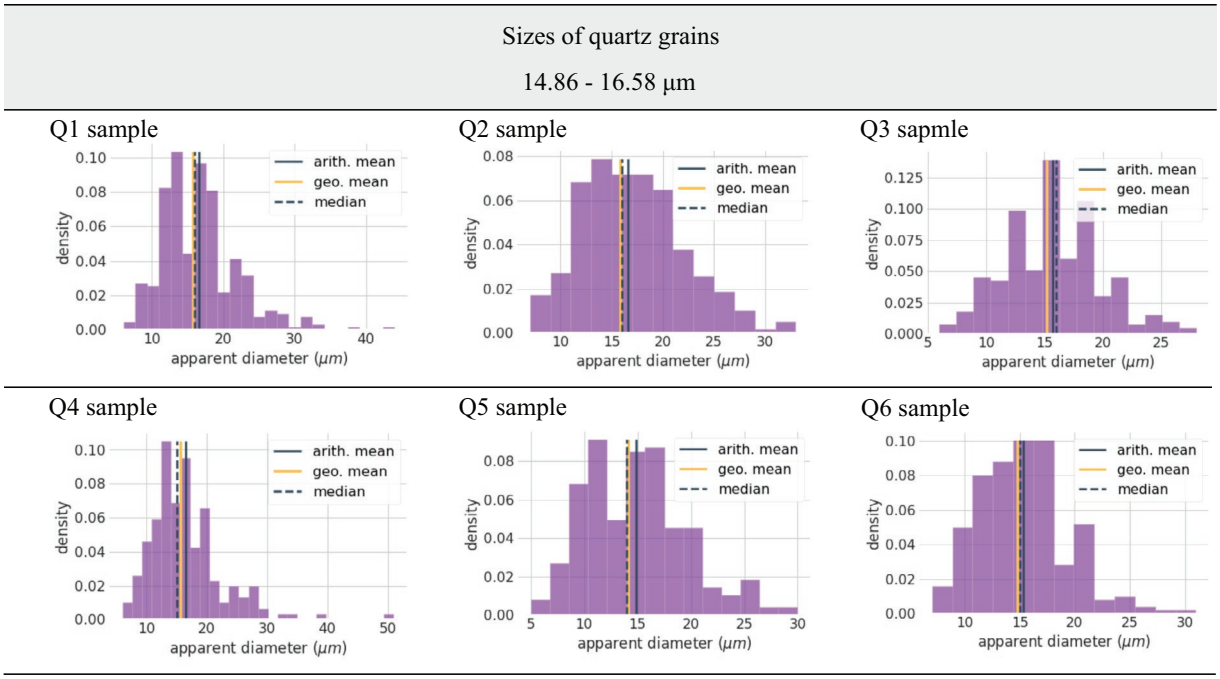

Fig. 9. Distribution of the quartz grain sizes in the dynamically-recrystallized aggregates of the quartzite mylonites.

the rocks composed mainly of quartz and feldspars, which are related to the orogen-parallel extension in the western part of the Veporic Unit, developed at increasing metamorphic conditions from 380 to 480 °C towards the structural footwall (Jeřábek et al. 2007).

Shear zones in the Veporic Unit were reactivated multiple times in the strike-slip regime (Jacko et al. 1996, 2001). This fact can be documented by a couple of shear band generations, as well as three different grain sizes of dynamically-recrystallized quartz in the aggregates of the mylonites of the crystalline rocks. Average grain-size diameters change depending on the microstructure where they occur (Figs. 7, 8, 9; Table 1). There is a significant change in grain size during dynamic recrystallization, which has been confirmed in many works in recrystallized, naturally- and experimentally-deformed rocks (Hirth & Tullis 1992; Stipp et al. 2002; Kilian et al. 2011). The size of dynamically-recrystallized grains is controlled mainly by the subgrain rotation recrystallization mechanism in all of the measured specimens. This mechanism occurs in a space where grain boundary migration is primarily driven by lattice strain energy (Hirth & Tullis 1992; Stipp & Kunze 2008; Platt & Behr 2011). Although temperature and water are factors influencing dynamic recrystallization, the grain size diameter is strongly dependent on differential stresses (e.g., Michibayashi 1993; Post & Tullis 1999; Stipp & Tullis 2003; Faleiros et al. 2010). The dynamically-recrystallized quartz aggregates with the coarser grains are parallel to the S planes, which correspond to the lowest differential stress values. The smallest grains in quartz aggregates and the higher differential stress values are related to the shear bands, which are younger and transect older S planes. Sizes of the dynamically-recrystallized grains in metaquartzite mylonites coincide with those in the wide shear bands (Table 1).

The structural record in the mylonites of the eastern part of the Veporic Unit is similar to that described in its western part. The difference is the general NW–SE strike of the shear zones and the geological units (Fig. 2). There are strongly-visible, subhorizontal stretching lineations of the above-mentioned direction present in all mylonitic rocks of the area. No other relics of the ductile lineations of different directions were observed. Shear zones are 10 to more than 100 m wide, and the ductile deformation in the low-grade metamorphic conditions is typical of them. The above-mentioned facts may point to the formation of the shear zone's structural pattern in an orogen-parallel extension regime (Jeřábek et al. 2007).

Conclusions

The contact between the Gemeric and the Veporic units, as well as the Margecany shear zone, belongs to important tectonic boundaries in the eastern part of the Central Western Carpathians. A set of the sub-parallel mylonite zones occurs in the adjacent part of the Veporic Unit, northwest of the tectonic zone. They tectonically separate the Veporic basement complexes from each other. The deformation across the area of the shear zone system can be characterized as follow:

- Shear zones are wide, exhumed zones of mylonites. Alpine deformation in the shear zones occurred in low-grade metamorphic conditions.
- Deformation in the shear zones was multi-phase with the development of a few subsequent foliation structures.

- Penetrative subhorizontal stretching lineation on the foliation planes of all mylonites indicates stretching and oriented ductile flow in a NW–SE direction.
- Microscopic, as well as macroscopic shear sense indicators show uniform, top-to-the-SE subhorizontal strike-slip movement of the shear zones hanging walls in the region.
- Microfabric of the mylonites of the crystalline rocks shows a slight increase in the intensity of the deformation towards the structural footwall of the units.
- The size of grains in the aggregates of dynamically-recrystallized quartz and the value of differential stress change, depending on the microstructure of which they are a part.
- The average size of quartz grains in dynamically-recrystallized aggregates parallel to S planes is 37.31–42.09 μm (Table 1). Quartz grains reach sizes of 14.89–16.89 μm in wide shear bands (Table 1).
- The dynamically-recrystallized quartz aggregates with the lowest differential stress value (33.57–37.12 MPa; Table 1) are parallel to S planes. Higher values of the differential stress (69.01–76.25 MPa; Table 1) are related to the wide shear bands, which are younger structures transecting S planes.
- The overall structural pattern of the mylonites indicates their development in orogen-parallel extension conditions.

Acknowledgments: This article was created with the support of VEGA grant 1/0585/20.

References

Berthé D., Choukroune P. & Jegouzo P. 1979: Orthogneiss, mylonite and non-coaxial deformation of granites: the example of the South Armoricain shear zone. *Journal of Structural Geology* 1, 31–42. https://doi.org/10.1016/0191-8141(79)90019-1

Biely A., Bezák V., Elečko M., Kaličiak M., Konečný V., Lexa J., Mello J., Nemčok J., Potfaj M., Rakús M., Vass D., Vozár J. & Vozárová A. 1996: Geological map of Slovakia 1:500 000. *Geological Survey of Slovak Republic*, Bratislava.

Bird P.C., Cartwright J.A. & Davies T.L. 2015: Basement reactivation in the development of rift basins: an example of reactivated Caledonide structures in the West Orkney Basin. *Journal of the Geological Society* 172, 77–85. https://doi.org/10.1144/jgs2013-098

Bónová K., Broska I. & Petrík I. 2010: Biotite from Čierna hora Mountains granitoids (Western Carpathians, Slovakia) and estimation of water contents in granitoid melts. *Geologica Carpathica* 61, 3–17. https://doi.org/10.2478/v10096-009-0040-1

Bukovská Z., Jeřábek P., Lexa O., Konopasek J., Janák M. & Košler J. 2013: Kinematically unrelated C-S fabrics: An example of extensional shear band cleavage from the Veporic Unit (Western Carpathians). *Geologica Carpathica* 64, 103–116. https://doi.org/10.2478/geoca-2013-0007

Burg J.P., Van Den Driessche J. & Brun J.P. 1994: Syn- to post-thickening extension: mode and consequences. *Comptes Rendus de l'Academie des Sciences, Serie II* 319, 1019–1032.

Chester F.M. 1989: Dynamic recrystallization in semi-brittle faults. *Journal of Structural Geology* 11, 847–858. https://doi.org/10.1016/0191-8141(89)90102-8

Christie J.M., Ord A. & Koch P.S. 1980: Relationship between recrystallized grain size and flow stress in experimentally defined quartzite. *EOS Transactions* 61, 377.

Dewey J.F., Shackleton R.M., Chang C.F. & Sun Y.Y. 1988: The tectonic evolution of the Tibetan Plateau. *Philosophical Transactions of the Royal Society, Series A: Mathematical, Physical and Engineering Sciences* 327, 379–413.

Ellis M. & Watkinson A.J. 1987: Orogen-parallel extension and oblique tectonics: The relation between stretching lineations and relative plate motions. *Geology* 15, 1022–1026. https://doi.org/10.1130/0091-7613(1987)15<1022:OEAOTT>2.0.CO;2

Etheridge M.A. & Wilkie J.C. 1981: An assessment of dynamically recrystallized grainsize as a palaeopiezometer in quartz-bearing mylonites zones. *Tectonophysics* 78, 475–508. https://doi.org/10.1016/0040-1951(81)90025-1

Faleiros F.M., Campanha G.A.C, Bello R.M.S & Fuzikawa K. 2010: Quartz recrystallization regimes, c-axis texture transitions and fluid inclusion reequilibration in a prograde greenschist to amphibolite facies mylonite zone (Ribeira Shear Zone, SE Brazil). *Tectonophysics* 485, 193–214. https://doi.org/10.1016/j.tecto.2009.12.014

Farkašovský R. 2013: Shear zones and mylonite microfabric in the Čierna hora Mts. (Eastern Slovakia). *Líceum Kiadó Eger*, 1–58.

Farkašovský R., Bónová K. & Košuth M. 2016: Microstructural, modal and geochemical changes as a result of granodiorite mylonitisation – a case study from the Rolovská shear zone (Čierna hora Mts, Western Carpathians, Slovakia). *Geologos* 22, 171–190. https://doi.org/10.1515/logos-2016-0019

Fitz Gerald J.D, Mancktelow N.S, Pennacchioni G. & Kunze K. 2006: Ultrafine-grained quartz mylonites from high-grade shear zones: Evidence for strong dry middle to lower crust. *Geology* 34, 369–372. https://doi.org/10.1130/G22099.1

Fossen H. 2016: Structural Geology. Second ed., *Cambridge University Press*, Cambridge, 1–509.

Fossen H. & Cavalcante G.C.G. 2017: Shear zones – A review. *Earth-Science Reviews* 171, 434–455. https://doi.org/10.1016/j.earscirev.2017.05.002

Fusseis F., Handy M.R. & Schrank C. 2006: Networking of shear zones at the brittle-to-viscous transition (Cap de Creus, NE Spain). *Journal of Structural Geology* 28, 1228–1243. https://doi.org/10.1016/j.jsg.2006.03.022

Gapais D. & White S.H. 1982: Ductile shear bands in a naturally deformed quartzite. *Textures and Microstructures* 5, 1–17. https://doi.org/10.1155/TSM.5.1

Gazdačko Ľ. 1994: Polyphase deformational development in the eastern part of contact zone of Gemericum and Veporicum (Western Carpathians). *Mineralia slovaca* 26, 387–398.

Guermani A. & Pennacchioni G. 1998: Brittle precursors of plastic deformation in a granite: an example from the Mont Blanc Massif (Helvetic, western Alps). *Journal of Structural Geology* 20, 135–148. https://doi.org/10.1016/S0191-8141(97)00080-1

Hirth G. & Tullis J. 1992: Dislocation creep regimes in quartz aggregates. *Journal of Structural Geology* 14, 145–159. https://doi.org/10.1016/0191-8141(92)90053-Y

Indares A., Dunning G. & Cox R. 2000: Tectono-thermal evolution of deep crust in a Mesoproterozoic continental collision setting: the Manicouagan example. *Canadian Journal of Earth Sciences* 37, 325–340. https://doi.org/10.1139/e99-069

Jacko S. 2007: Successive relationships of tectonometamorphic parageneses in the Branisko and Čierna hora Mts. (Western Carpathians). *Acta Geologica Universitatis Comenianae* 1, 33–40.

Jacko S., Korikovskij S.P. & Boronichin V.A. 1990: Rovnovážne asociácie rúl a amfibolitov komplexu Bujanovej (Čierna hora). *Mineralia slovaca* 22, 231–239.

Jacko S., Sasvári T., Zacharov M., Schmidt R. & Vozár J. 1996: Contrasting styles of Alpine deformations at the eastern part of the Veporicum and Gemericum units, Western Carpathians. *Slovak Geological Magazine* 2, 151–164.

Jacko S., Farkašovský R. & Schmidt R. 2001: Veporic basement of the Branisko and Čierna hora Mts.: an example for Hercynian and Alpine polystage evolution. In: Bezák V., Siman P., Madarás P. & Broska I. (eds.): Proceedings of the Western Carpathian and European Hercynides. *State Geological Institute of Dionyz Štúr*, Bratislava, 18–20.

Janák M., Plašienka D., Frey M., Cosca M., Schmidt S.Th., Lupták B. & Méres Š. 2001: Cretaceous evolution of a metamorphic core complex, the Veporic unit, Western Carpathians (Slovakia): P–T conditions and in situ $^{40}Ar/^{39}Ar$ UV laser probe dating of metapelites. *Journal of Metamorphic Geology* 19, 197–216. https://doi.org/10.1046/j.0263-4929.2000.00304.x

Jeřábek P., Stünitz H., Heilbronner R., Lexa O. & Schulmann K. 2007: Microstructural-deformation record of an orogen-parallel extension in the Vepor Unit, West Carpathians. *Journal of Structural Geology* 29, 1722–1743. https://doi.org/10.1016/j.jsg.2007.09.002

Jeřábek P., Faryad W.S., Schulmann K., Lexa O. & Tajčmanová L. 2008: Alpine burial and heterogeneous exhumation of Variscan crust in the West Carpathians: Insight from thermodynamic and argon diffusion modelling. *Journal of the Geological Society* 165, 479–498. https://doi.org/10.1144/0016-76492006-165

Jeřábek P., Lexa O., Schulmann K. & Plašienka D. 2012: Inverse ductile thinning via lower crustal flow and fold-induced doming in the West Carpathiann Eo-Alpine collisional wedge. *Tectonics* 31, 1–26. https://doi.org/10.1029/2012TC003097

Kilian R., Heilbronner R. & Stünitz H. 2011: Quartz grain size reduction in a granitoid rock and the transition from dislocation to diffusion creep. *Journal of Structural Geology* 33, 1265–1284. https://doi.org/10.1016/j.jsg.2011.05.004

Korikovskij S.P., Jacko S. & Boronichin V.A. 1989: Alpine anchimetamorphism of upper carboniferous sandstones from the sedimentary mantle of the Čierna hora Mts. crystalline complex (Western Carpathians). *Geologický Zborník Geologica Carpathica* 40, 579–598.

Korikovskij S.P., Jacko S. & Boronichin V. A. 1990: Faciálne podmienky variskej prográdnej metamorfózy v lodinskom komplexe kryštalinika Čiernej hory. *Mineralia slovaca* 22, 225–230.

Krist E., Korikovskij S. P., Putiš M., Janák M. & Faryad S. W. 1992: Geology and Petrology of Metamorphic Rocks of the Western Carpathians Crystalline Complexes. *Comenius University*, Bratislava, 1–324.

Lexa O., Schulmann K. & Ježek J. 2003: Cretaceous collision and indentation in the West Carpathians: View based on structural analysis and numerical modeling. *Tectonics* 22, art. no. 1066. https://doi.org/10.1029/2002TC001472

Lister G.S. & Snoke A.W. 1984: S-C mylonites. *Journal of Structural Geology* 6, 617–638. https://doi.org/10.1016/0191-8141(84)90001-4

Lopez-Sanchez M.A. 2018: GrainSizeTools: a Python script for grain size analysis and paleopiezometry based on grain size. *Journal of Open Source Software* 3, 863. https://doi.org/10.21105/joss.00863

Lopez-Sanchez M.A. & Llana-Fúnez S. 2015: An evaluation of different measures of dynamically recrystallized grain size for paleopiezometry or paleowattometry studies. *Solid Earth* 6, 475–495. https://doi.org/10.5194/se-6-475-2015

Mancktelow N.S. & Pavlis T.L. 1994: Fold-fault relationships in low-angle detachment systems. *Tectonics* 13, 668–685. https://doi.org/10.1029/93TC03489

Mercier J-C., Anderson D.A. & Carter N.L. 1977: Stress in the lithosphere: Inferences from steady state flow of rocks, *Pure and Applied Geophysics* 115, 199–226. https://doi.org/10.1007/BF01637104

Michibayashi K. 1993: Syntectonic development of a strain-independent steady-state grain size during mylonitization. *Tectonophysics* 222, 151–164. https://doi.org/10.1016/0040-1951(93)90046-M

Németh Z., Putiš M. & Grecula P. 2000: Tectonic evolution of Gemericum (the Western Carpathians) outlined by theresults of petrotectonic research. *Mineralia Slovaca* 32, 169–172.

Papeschi S., Musumeci G. & Mazzarini F. 2018: Evolution of shear zones through the brittle-ductile transition: The Calamita Schists (Elba Island, Italy). *Journal of Structural Geology* 113, 100–114. https://doi.org/10.1016/j.jsg.2018.05.023

Passchier C.W. & Simpson C. 1986: Porphyroclast systems as kinematic indicators. *Journal of Structural Geology* 8, 831–844. https://doi.org/10.1016/0191-8141(86)90029-5

Passchier C.W, Hoek J.D., Bekendam R.F. & De Boorder H.1990: Ductile reactivation of Proterozoic brittle fault rocks; an example from the Vestfold Hills, East Antarctica. *Precambrian research* 47, 3–16.

Passchier C.W. & Trouw R.A.J. 2005: Microtectonics. Second ed., *Springer*, Berlin, 1–366.

Paterson M.S. & Wong T.F. 2005: Experimental Rock Deformation – The Brittle Field. Second ed., *Spinger-Verlag*, New York, 1–348. https://doi.org/10.1007/b137431

Phillips T.B., Jackson C.A-L., Bell R.E., Duffy O.B. & Fossen H. 2016: Reactivation of intrabasement structures during rifting: A case study from offshore southern Norway. *Journal of Structural Geology* 91, 54–73. https://doi.org/10.1016/j.jsg.2016.08.008

Plašienka D. 1995: Passive and active margin history of the northern Tatricum (Western Carpathians, Slovakia). *Geologische Rundschau* 84, 748–760.

Plašienka D. 2003: Development of basement-involved fold and thrust structures exemplified by the Tatric-Fatric-Veporic nappe system of the Western Carpathians (Slovakia). *Geodinamica Acta* 16, 21–38. https://doi.org/10.1016/S0985-3111(02)00003-7

Plašienka D., Broska I., Kissová D. & Dunkl I. 2007: Zircon fission-track dating of granites from the Vepor-Gemer Belt (Western Carpathians): constraints for the Early Alpine exhumation history. *Journal of Geosciences* 52, 113–123. https://doi.org/10.3190/jgeosci.009

Platt J.P. & Behr W.M. 2011: Deep structure of lithospheric fault zones. *Geophysical Research Letters* 38. https://doi.org/10.1029/2011GL049719

Platt J.P. & Vissers R.L.M. 1980: Extensional structures in anisotropic rocks. *Journal of Structural Geology* 2, 397–410. https://doi.org/10.1016/0191-8141(80)90002-4

Polák M., Jacko S., Vozár J., Vozárová A., Gross P., Harčár J., Sasvári T., Zacharov M., Baláž B., Kaličiak M., Karoli S., Nagy A., Buček J., Maglay Z., Spišák Z., Žec B., Filo I. & Janočko J. 1996: Geological map of the Branisko and Čierna hora Mts. 1:50 000. *Geological Survey of Slovak Republic*, Bratislava.

Polák M., Jacko S., Vozárová A., Vozár J., Gross P., Harčár J., Zacharov M., Baláž B., Liščák P., Malík, P., Zakovič M., Karoli S. & Kaličiak M. 1997: Explanatory notes to the Geological map of the Branisko and Čierna hora Mts. 1:50 000. Bratislava. *State Geological Institute of Dionýz Štúr*, Bratislava, 1–201.

Post A. & Tullis J. 1999: A recrystallized grain size paleopiezometer for experimentally deformed feldspar aggregates. *Tectonophysics* 303, 159–173. https://doi.org/10.1016/S0040-1951(98)00260-1

Pryer L.L. 1993: Microstructures in feldspars from a major crustal thrust zone: the Grenville Front, Ontario, Canada. *Journal of Structural Geology* 15, 21–36. https://doi.org/10.1016/0191-8141(93)90076-M

Putiš M., Unzog W., Wallbrecher E. & Fritz H. 1997: Mylonitization and chemical mass-transfer in granitoid rocks of the Vepor pluton near the Cretaceous Pohorelá thrust (Veporic unit, central Western Carpathians). In: Grecula P., Hovorka D. & Putiš M. (Eds.): Geological Evolution of the Western Carpathians. *Mineralia Slovaca*, Bratislava, 197–214.

Ramsay J.G. 1980: Shear zone geometry: A review. *Journal of Structural Geology* 2, 83–99. https://doi.org/10.1016/0191-8141(80)90038-3

Ramsay J.G. & Graham R.H. 1970: Strain variation in shear belts. *Canadian Journal of Earth Sciences* 7, 786–813. https://doi.org/10.1139/e70-078

Ratschbacher L., Frisch W., Linzer H.-G. & Merle O. 1991: Lateral extrusion in the Eastern Alps: Part 2. Structural analysis. *Tectonics* 10, 257–271. https://doi.org/10.1029/90TC02623

Schmid S.M., Paterson M.S. & Boland J.N. 1980: High temperature flow and dynamic recrystallization in Carrara marble. *Tectonophysics* 65, 245–280. https://doi.org/10.1016/0040-1951(80)90077-3

Scholz C.H. 1988: The brittle-plastic transition and the depth of seismic faulting. *Geologische Rundschau* 77, 319–328.

Sibson R.H. 1977: Fault rocks and fault mechanisms. *Journal of the Geological Society* 133, 191–213. https://doi.org/10.1144/gsjgs.133.3.0191

Simpson C. 1985: Deformation of granitic rocks across the brittle-ductile transition. *Journal of Structural Geology* 7, 503–511. https://doi.org/10.1016/0191-8141(85)90023-9

Stipp M. & Kunze K. 2008: Dynamic recrystallization near the brittle-plastic transition in naturally and experimentally deformed quartz aggregates. *Tectonophysics* 448, 77–97. https://doi.org/10.1016/j.tecto.2007.11.041

Stipp M. & Tullis J. 2003: The recrystallized grain size piezometer for quartz. *Geophysical Research Letters* 30. https://doi.org/10.1029/2003GL018444

Stipp M., Stünitz H., Heilbronner R. & Schmid S.M. 2002: The eastern Tonale fault zone: a 'natural laboratory' for crystal plastic deformation of quartz over a temperature range from 250 to 700 °C. *Journal of Structural Geology* 24, 1861–1884. https://doi.org/10.1016/S0191-8141(02)00035-4

Stipp M., Fügenschuh B., Gromet L.P., Stünitz H. & Schmid S.M. 2004: Contemporaneous plutonism and strike-slip faulting: A case study from the Tonale fault zone north of the Adamello pluton (Italian Alps). *Tectonics* 23. https://doi.org/10.1029/2003TC001515

Stünitz H. 1998: Syndeformational recrystallization-dynamic or compositionally induced? *Contributions to Mineralogy and Petrology* 131, 219–236. https://doi.org/10.1007/s004100050390

ten Grotenhuis S.M., Trouw R.A.J. & Passchier C.W. 2003: Evolution of mica fish in mylonitic rocks. *Tectonophysics* 372, 1–21. https://doi.org/10.1016/S0040-1951(03)00231-2

Twiss R.J. 1977: Theory and applicabitily of recrystallized grain size paleopiezometer. *Pure and Applied Geophysics* 115, 227–244. https://doi.org/10.1007/BF01637105

Viegas G., Menegon L. & Archanjo C. 2016: Brittle grain-size reduction of feldspar, phase mixing and strain localization in granitoids at mid-crustal conditions (Pernambuco shear zone, NE Brazil). *Solid Earth* 7, 1–22. https://doi.org/10.5194/se-7-375-2016

Vojtko R., Králiková S., Jeřábek P., Schuster R., Danisik M., Fügenschuh B., Minár J. & Madarás J. 2016: Geochronological evidence for the Alpine tectono-thermal evolution of the Veporic Unit (Western Carpathians, Slovakia). *Tectonophysics* 666, 48–65. https://doi.org/10.1016/j.tecto.2015.10.014

Vozárová A. & Vozár J. 1988: Late Paleozoic in West Carpathians. *State Geological Institute of Dionýz Štúr*, Bratislava, 1–314.